



# The soil pore structure encountered by roots affects plant-derived carbon inputs and fate

Maik Lucas<sup>1,2</sup>, James P. Santiago<sup>3</sup>, Jinyi Chen<sup>4</sup>, Andrey Guber<sup>1</sup> and Alexandra Kravchenko<sup>1</sup>

Department of Plant, Soil and Microbial Sciences, DOE Great Lakes Bioenergy Research Center, Michigan State University, East Lansing, MI 48824, USA; Department of Soil System Sciences, Helmholtz Centre for Environmental Research – UFZ, Halle (Saale), 06110, Germany; <sup>3</sup>Plant Resilience Institute and MSU-DOE Plant Research Laboratory, Michigan State University, East Lansing, MI 48824, USA; <sup>4</sup>Department of Plant Protection, Nanjing Agricultural University, Nanjing, 210095, China

Author for correspondence: Maik Lucas

Email: maik.lucas@ufz.de

Received: 12 May 2023 Accepted: 5 July 2023

New Phytologist (2023) 240: 515-528 doi: 10.1111/nph.19159

Key words: carbon allocation, carbon sequestration, pore structure, root-soil contact, X-ray computed tomography.

## **Summary**

- Plant roots are the main supplier of carbon (C) to the soil, the largest terrestrial C reservoir. Soil pore structure drives root growth, yet how it affects belowground C inputs remains a critical knowledge gap.
- By combining X-ray computed tomography with <sup>14</sup>C plant labelling, we identified root–soil contact as a previously unrecognised influence on belowground plant C allocations and on the fate of plant-derived C in the soil.
- Greater contact with the surrounding soil, when the growing root encounters a pore structure dominated by small ( $< 40 \,\mu m \, \varnothing$ ) pores, results in strong rhizodeposition but in areas of high microbial activity. The root system of Rudbeckia hirta revealed high plasticity and thus maintained high root-soil contact. This led to greater C inputs across a wide range of soil pore structures. The root-soil contact Panicum virgatum, a promising bioenergy feedstock crop, was sensitive to the encountered structure. Pore structure built by a polyculture, for example, restored prairie, can be particularly effective in promoting lateral root growth and thus rootsoil contact and associated C benefits.
- · The findings suggest that the interaction of pore structure with roots is an important, previously unrecognised, stimulus of soil C gains.

#### Introduction

Approximately 1:3 of the carbon (C) photo-assimilated by plants from the atmosphere is transferred belowground (Jones et al., 2009; Pausch & Kuzyakov, 2018), making the Earth's soils a massive C reservoir (Friedlingstein et al., 2022). The lion's share of these inputs, however is being lost to the atmosphere as CO2, with only c. 5% of the total photo-assimilated C remaining in the soil (Jones et al., 2009; Pausch & Kuzyakov, 2018), and most of what remains are further degraded by microbes over time. Live root inputs via rhizodeposition, that is, mucilage, root cap cells, exudates, and lysates, are an important component of stable soil organic matter (Rasse et al., 2005; Gherardi & Sala, 2020; Gregory, 2022). Such inputs can be 2-13 times more efficient than inputs from dead roots, aka root litter, in generating both the rapidly utilisable C and the slowly metabolised mineral-associated C (Sokol et al., 2019). Maximising the live root inputs is a viable strategy for increasing the mean residence time of soil C (Poeplau et al., 2021).

Plant species differ, sometimes substantially, in their soil C inputs and their effects on soil C cycling, due to a variety of factors, with perenniality, C<sub>3</sub>: C<sub>4</sub> status, and root architecture just a few to mention. Many species-related root traits, for example, root lengths, diameters, and branching, are particularly important for soil C inputs as well as C stabilisation (Poirier et al., 2018). However, they are

typically investigated under controlled conditions, such as wellsieved soil, potting soil mixtures, or litter bags, and not in soils with intact structures (Poirier et al., 2018). Yet, it is the local variations in structural properties encountered by the roots as they navigate through the intact soil that greatly affects root growth patterns and architecture (Colombi et al., 2018; Lucas, 2022). How such local variations influence the quantities of C that a root puts underground remains largely enigmatic.

Soil pore structure, that is, size distributions, shapes, and connectivity of soil pores (Rabot et al., 2018), can affect root-derived C inputs and their fate in multiple ways. First, pore structure interacts with root growth. This interaction is mutual where roots change the structure of soil pores, but also, the pore structure changes root growth (Lucas et al., 2019a). A root can grow along pores larger than its size, encountering little resistance and thus navigating soil layers with high bulk density without marked changes to an existing arrangement of soil pores (White & Kirkegaard, 2010; Gao et al., 2016; Lucas et al., 2019a). Alternatively, a root can grow into a dense soil matrix, overcoming the penetration resistance, and reorganising the pore space as it goes, resulting in the densification of its immediate surroundings and creating biopores upon its death and decomposition (Bruand et al., 1996; Lucas et al., 2019b).

These different modes of interaction between roots and pore structure have profound effects on the rhizosphere (Vetterlein

et al., 2020; Lucas, 2022) and define where within the soil matrix the root C inputs are deposited and how physically accessible they are for subsequent microbial decomposition (Erktan et al., 2020). The impacts of such interactions are very complex and sometimes contradictory. For example, plant-accessible pores in the few tens of µm size range can receive large quantities of plant-derived C (Quigley et al., 2018; Quigley & Kravchenko, 2022). The abundance and connectivity of such pores enable enhanced root growth, as observed in many well-structured soils, and subsequent high cumulative C inputs benefit soil C gains (Dexter, 1991; Stirzaker et al., 1996; Colombi et al., 2019). But, on the other hand, an absence of easily accessible pores can also lead to elevated C inputs, since roots grown into dense poorly-structured soil matrix increase rhizodeposition via mucilage production (Iijima & Kono, 1992; Jones et al., 2009). To further complicate the matters, root exudates, a substantial part of all rhizodeposits, are released passively, responding to root-to-soil gradients (Jones et al., 2009). Hence, their quantities might be stimulated by better root contact with the surrounding soil matrix, also largely a function of soil pore structure.

The goal of this study is to explore how root interactions with the soil pore structure affect the additions of photo-assimilated C to the soil and the fate of the added C. We hypothesise that plant species with disparate root architectures may naturally differ in how they react to a specific pore structure with disparate consequences for C inputs and protection. Thus, we selected two plant species with distinctly different root characteristics, namely Rudbeckia hirta (black-eyed Susan) and Panicum virgatum (switchgrass, Fig. 1a). The short-lived perennial forb R. hirta is an Asteraceae, with a fibrous root system and a large amount of small laterals (Levang-Brilz & Biondini, 2003). P. virgatum is a perennial grass with a massive, coarse root system and low root branching (Weaver, 1968; McLaughlin & Adams Kszos, 2005). While P. virgatum can have a tremendous effect on soil pore structure (Juyal et al., 2021), the small roots of R. hirta might not affect it in a measurable way (Judd et al., 2015).

The detailed characterisation of the soil pore structure, quantification of the new root growth within it, and assessments of the pore characteristics of the rhizosphere created by the ingrowing roots were made possible by the use of X-ray computed microtomography ( $\mu$ CT). Labelling the growing plants with <sup>14</sup>C enabled us to explore multiple aspects of new C additions. Specifically, we assessed the quantities of plant-derived C inputs; traced localities of the new C placement within rhizosphere, rhizoplane (i.e. root surfaces), roots, and in the soil solution from pores of different size ranges; monitored losses of newly added C as  $CO_2$  and quantified the amounts of newly added C remaining in the soil (Fig. 1b).

#### **Materials and Methods**

#### Study area and sampling

The experimental site used in this study was established in 2013 in Oregon, WI, USA in a randomised complete block design with four replications. The soil samples were taken from two

vegetation systems: monoculture switchgrass (variety Cave-inrock) and restored prairie (an 18-species mix including *Panicum virgatum* L. and *Rudbeckia hirta* L. along with other forbs, grasses, and legumes). It has been demonstrated that after multiple years of uninterrupted growth the vegetation communities of the two systems can develop distinctly different soil pore characteristics (Kravchenko *et al.*, 2019), providing pore structure contrast needed for this study. Please refer to Supporting Information Methods S1 for additional details on the soil sampling and the design and management of the experiment.

To create a variety of contrasting pore structures, we generated four types of ingrowth cores (15 cores of each type): namely, intact and sieved cores from each of the switchgrass and prairie system. All ingrowth cores were held by perforated covers with large perforations (4 mm Ø) to not inhibit root growth (Fig. S1d-f). The intact ingrowth cores were prepared by taking them out of their original field holders and enclosing them within the perforated covers. The sieved cores were prepared by sieving individual field cores (2 mm) and then repacking their soil into perforated covers. Sieving drastically affected pore characteristics, thus greatly expanding the range of pore structures for the study, yet, it did not change other soil properties. To ensure that the intact and sieved cores differ only in terms of their pore structure, all roots and stones from the original field soil core collected on the sieve were mixed back before repacking.

#### Experimental design

For the plant growth experiment, 12 pots (15 cm Ø and 20 cm height) were filled with sieved soil (see Methods S1) to  $1.34\,\mathrm{g\,cm^{-3}}$  bulk density, the average bulk density measured in the field. During the filling process, four ingrowth cores representing every combination of soil structure (sieved vs intact) and soil origin (switchgrass vs prairie-soil) were placed into the pots at 10-15 cm depth (Figs 1a, S1f). The use of the ingrowth cores enabled us to achieve high resolution of the µCT scans, providing pore structure data of high quality. At the same time, keeping the ingrowth cores within large pots ensured unrestricted root growth. Our experimental settings can be regarded as a split-root design, where exposing the cores with different pore structures to the roots of the same plant minimised variations due to plant effects, for example, plant development stages or photo-assimilation rates. The cores were placed to ensure they were within the same depth of the pot and at the same distances to the pot walls.

Pre-germinated seedlings were planted into the centres of the pots at an equal distance to all ingrowth cores. The plants were grown for 48 d in a growth chamber. Detailed information on the growing conditions is provided in Methods S2.

# <sup>14</sup>C labelling

In order to assess the quantities, locations, and decomposition losses of the photo-assimilated C added by plants to the ingrowth cores with contrasting pore structures, we labelled the plants with <sup>14</sup>C–CO<sub>2</sub> according to Santiago *et al.* (2021). Briefly, LI-COR 6800 portable photosynthesis system (Li-Cor, Lincoln, NE,

2, Dowloaded from https://nph.onlinelbrary.wiley.com/doi/10.1111/nph.19159, Wiley Online Library on [22/09/2023]. See the Terms and Conditions (https://onlinelbbrary.wiley.com/terms-and-conditions) on Wiley Online Library for rules of use; OA articles are governed by the applicable Creative Commons Licens

**Fig. 1** Outline of the experimental design and analytical methods used in this study. (a) *Rudbeckia hirta* and *Panicum virgatum* were planted into containers filled with 2-mm sieved soil (Supporting Information Fig. S1a–c) and holding perforated cores with soil of four contrasting pore structure characteristics (Fig. S1d–f), namely: intact and sieved soils of prairie and switchgrass origin. To ensure that the intact and sieved cores differed from each other only in terms of pore structure, the sieved soil was packed to the same bulk density as the intact cores and all > 2 mm inclusions, such as stones and large root residues were incorporated back into the sieved soil before packing. (b)  $^{14}$ C pulse labelling of the growing plants (Fig. S1g) enabled tracing  $^{14}$ C into root: soil compartments and its distribution within the soil (Fig. S1h) as well as to assess the short-term fate of the newly added C as  $^{14}$ CO<sub>2</sub>, dissolved  $^{14}$ C in the soil solution in pores of two contrasting sizes (Fig. S1i), and the total  $^{14}$ C remaining within the soil. (c) X-ray  $\mu$ CT imaging before and after the experiment allowed characterisation of pore size distributions, identification of biopores, and quantification of undecomposed plant residues, for example, old roots within the cores (grey), together enabling investigation of how new roots (brown) explored different pore structures and how their exploration patterns defined physical properties of the rhizosphere. Note that the black areas within larger biopores result from cutting these at the edge of the picture.

USA) with an attached  $3 \times 3$  cm chamber was used to feed plant leaf's with CO2 (Fig. S1g). For P. virgatum two to three leaf blades were laid side by side and clamped into the chamber. Leaves of R. hirta were large enough to fill the whole chamber, and only one fully mature leaf was clamped. Before labelling, stable photosynthetic rates were achieved by feeding the leaves with unlabelled CO<sub>2</sub>. For feeding with labelled CO<sub>2</sub>, a constant flow from a pressurised <sup>14</sup>CO<sub>2</sub> tank ensured a concentration of 420  $\mu$ mol mol<sup>-1</sup> of labelled CO<sub>2</sub> in the chamber. The pressurised tank contained 5% unlabelled CO2 in O2 mixed with <sup>14</sup>C-CO<sub>2</sub>, created by acidifying NaH<sup>14</sup>CO<sub>3</sub>. The final radioactivity of <sup>14</sup>CO<sub>2</sub> used was 1 Bq mmol<sup>-1</sup>. To ensure a distribution of <sup>14</sup>C in the whole root system (Pausch & Kuzyakov, 2011) as well as sufficient amounts of detectable <sup>14</sup>C in the rhizosphere, the plants were labelled 11 d and 3 d before harvest. The photosynthetic activity was logged every 5 min and used to calculate the total radioactivity taken up by the plant over the labelling time of 2.5 h. Both plants took up <sup>14</sup>C in the amounts sufficient for the subsequent analysis (Table S1).

# Harvest and <sup>14</sup>C analyses

During the harvest, the aboveground plant tissue was collected, cut into pieces and dried (60°C) overnight. The pots were cut

open, and the ingrowth cores were carefully removed, with ingrowing roots carefully cut-out at the core surfaces.

The upper cap of the cores was removed, and two intact soil samples (2 cm Ø and 2.5 cm height) were taken into plastic tubes and pushed into the soil (Fig. 1b). One of the two samples was used for quantifying <sup>14</sup>C with the soil solution. The centrifugation method (Russell & Richards, 1939) enabled us to derive soil solution from two different pore size classes with equivalent diameters of > 35 µm (referred here to DOC from macropores  $>\!40\,\mu m$  Ø) and 2–35  $\mu m$  (referred here to DOC from small pores < 40 µm Ø). While the first size class is associated with increased microbial activity, the latter was shown to be important for C storage (Bouckaert et al., 2013; Kravchenko & Guber, 2017; Kravchenko et al., 2019). The other intact soil sample was used for determining <sup>14</sup>C-CO<sub>2</sub> losses during 30-d soil incubation. Note that to ensure precise <sup>14</sup>C-CO<sub>2</sub>-analyses, we did not measure total CO2 release on a subsample of the trapping solution and could, therefore, not capture priming effects, that is, the release of native C through increased microbial activity.

To explore where else within the soil (aside from the rhizosphere) the newly added <sup>14</sup>C was deposited, we collected nine microsamples (0.1 cm<sup>3</sup>) from referenced locations within each intact soil core. The microsamples were taken on a regular square grid (Fig. S1h) and are referred to further on as <sup>14</sup>C grid samples (Figs 1b, S1h).

The remaining soil of the ingrowths cores was used to procure the ingrown roots in order to characterise <sup>14</sup>C of the root tissues, rhizoplane, and rhizosphere. The roots were carefully taken out of the remaining soil with tweezers, and rhizosphere and rhizoplane fractions were obtained following the procedures described by Lucas *et al.* (2018).

For details on the sampling procedure as well as the radioactivity evaluation, see Methods S3. The <sup>14</sup>C activities of each compartment (e.g. rhizosphere and root) in different cores are normalised based on the total assimilated <sup>14</sup>C of the plant within a given container to describe the relative pathways of the added <sup>14</sup>C-label. To ensure that the <sup>14</sup>C-activities are not misinterpreted due to differences in root growth, we also present data based on the length of the roots found within each core.

## X-ray µCT scanning and image analyses

All intact and sieved ingrowth cores were μCT scanned twice – before and after the ingrowth experiment at a resolution of 18.2 μm. The images were reconstructed following the procedures from Lucas *et al.* (2022). To follow the root growth path, the μCT images taken before and after the growth experiment were registered using elastix (Klein *et al.*, 2010; Shamonin, 2013) as described in Lucas *et al.* (2020a). After the registration, 1850 × 1850 × 2300 voxel cubes were cut from the centres of the cores' images in FiJi (Ollion *et al.*, 2013) to remove artefacts along the core walls. In addition, a contrast enhancement (saturation value of 0.35) was performed, and the bit depth was reduced to 8-bit. After this, a non-local means filter was used (Darbon *et al.*, 2008; Buades *et al.*, 2011) with scikit-image (van der Walt *et al.*, 2014) in PYTHON (van Rossum & Drake, 2009).

Lucas et al. (2020b) showed that to representatively describe pore volumes, the pores need to have a diameter two to three times the scanning resolution. Thus, we focused on pores  $> 40 \,\mu m$  Ø, hereafter referred to as macropores, while soil volumes dominated by pores  $\leq 40 \,\mu\text{m}$  Ø, hereafter, will be referred to as soil matrix. For pore segmentation, we used the Otsu algorithm (Otsu, 1979). Biopores and roots were segmented according to the workflow of Lucas et al. (2022). The respective IMAGEJ scripts can be found on 'https://github.com/Maik-Lu/Roots\_and\_Biopores'. See Methods S4 and Fig. S2 for details on the root segmentation approach. To assess pore characteristics of the soil matrix, that is, < 40 µm pores, we conducted µCT scanning and subsequent analyses of several intact subsamples at c. 5 µm resolution. For that, three intact subsamples (0.8 cm Ø and 0.8 cm height) were taken from an additional set of intact cores of both vegetation systems and subjected to X-ray µCT scanning at the Advanced Photon Source (APS), Argonne National Laboratory (scanning and analyses details are provided in Methods \$5).

By identifying the root residues in the  $\mu$ CT scans of intact ingrowth cores before the experiment and then examining the same residues on the scans obtained after the experiment, we were able to quantify the residue decomposition and relate it to the properties of the surrounding soil. Newly grown roots were separated from the old root residues by image subtraction (Fig. 1c). The volume of degraded old roots was obtained by subtracting

the root image after the experiment, that is, with only new roots and degraded root residues, from the root image before the experiment, that is, with non-degraded root residues.

Pore size distribution (PSD) and pore connectivity were obtained from the pore binary images. To compute the PSD in Fiji, the local thickness method (Hildebrand & Rüegsegger, 1997) was used. A size thresholding on the PSD (pores larger than 0.1 mm) was labelled using the connected component labelling from the plugin BoneJ2 plugin (v.7.10, Domander *et al.*, 2021). This image was used to calculate the  $\Gamma$ -indicator, a metric of pore connectivity (Lucas *et al.*, 2020b).

To describe in which pore structure roots grew, the image of the newly grown roots was used as a mask on the segmented image from before the experiment. The physical properties of the rhizosphere were calculated using the Euclidean Distance Transform in Fiji, as shown in Lucas *et al.* (2019a). To determine root–soil contact, we calculated mean values (total macropore, matrix and narrow macropore volume, i.e. pores < 150  $\mu$ m Ø) as percentages of the total volume of the rhizosphere up to 0.1 mm distance to the root surfaces. This distance was determined from iterative comparing the correlation of soil matrix density with  $^{14}$ C measurements, accounting for root–soil contact changes due to root shrinkage (Koebernick *et al.*, 2018).

#### **Statistics**

The data were analysed using a linear mixed model approach implemented in the LME4-package (Bates et al., 2015) of R (v.4.1.1). The statistical model consisted of fixed effects of the plant (P. virgatum vs R. hirta), soil structure (sieved vs intact), and soil origin (switchgrass-soil vs prairie-soil) and their interactions. The random effects consisted of the planted pots, used as an error term for testing the plant effect, and of the ingrowth cores nested within the pots, used as an error term for testing the effects of the soil structure and origin. The assumptions of normality and homogeneity of variances were assessed using normal probability plots of the residuals and Levene's tests for equal variances, respectively. When the normality assumption was found to be violated, the data were log-transformed (as in the case of all <sup>14</sup>C results). When the interactions between the studied factors were found to be statistically significant (P<0.05), slicing of the interaction, aka simple effect F-tests, were conducted, followed, when significant, by t-tests for multiple comparisons among the mean values.

## **Results**

#### The effect of pore structure on root growth

After 8 yr of implementation, soils taken from the two perennial plant systems diverged in their biological and structural characteristics but remained similar in terms of chemical composition (Table S2). The sieved cores exhibited significantly higher macroporosity than the intact cores (*c.* 20% vs 5%) (Fig. S3a), with a large proportion of narrow (40–150 µm Ø) macropores (Fig. S3c) but similar pore connectivity (Fig. S3b). The capability

2, Downloaded from https://nph.onlinelibrary.wiley.com/doi/10.1111/nph.19159, Wiley Online Library on [22/09/2023]. See the Terms and Conditions (https://onlinelibrary.wiley.com/terms-and-conditions) on Wiley Online Library for rules of use; OA articles are governed by the applicable Creative Commons Licens

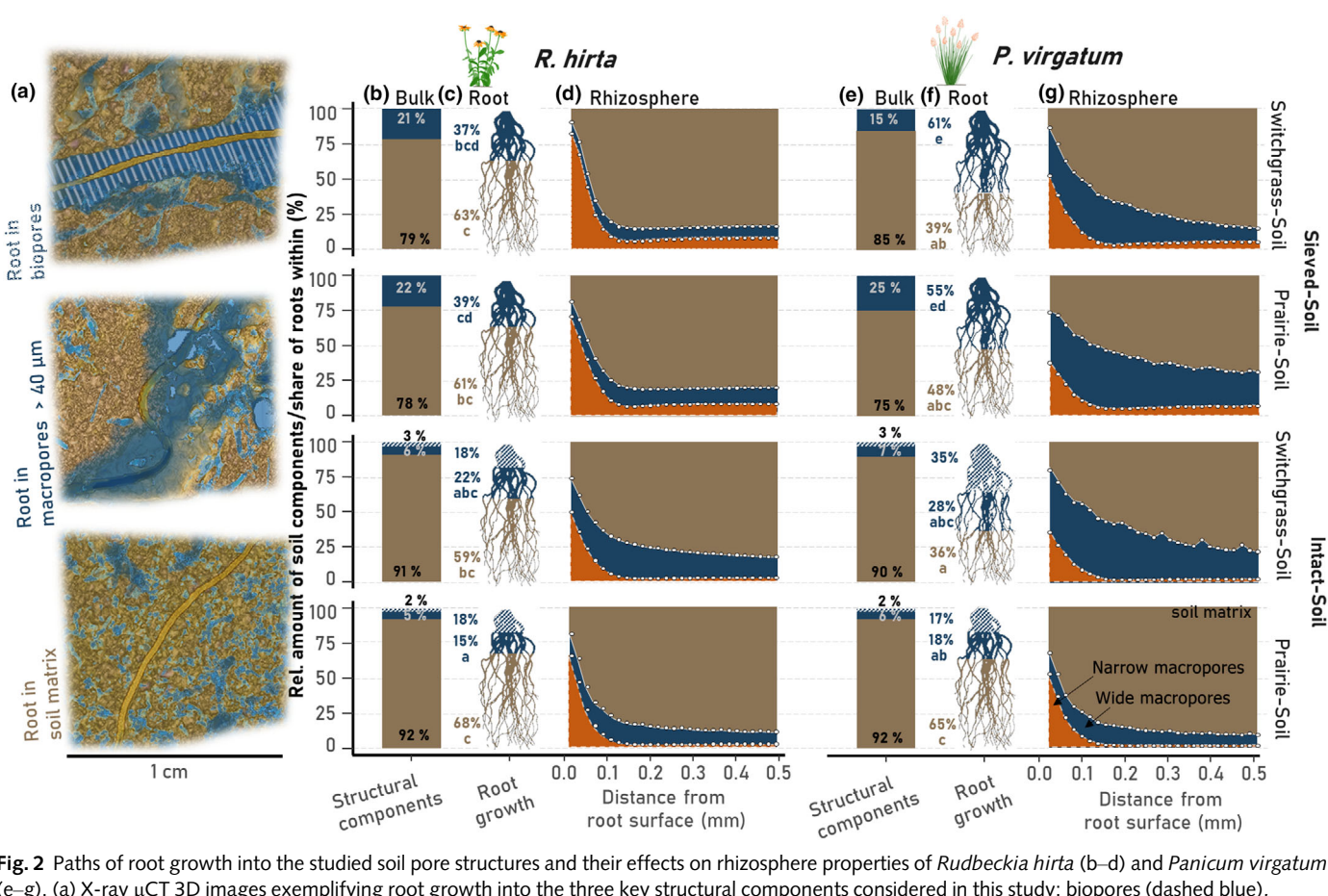


Fig. 2 Paths of root growth into the studied soil pore structures and their effects on rhizosphere properties of Rudbeckia hirta (b-d) and Panicum virgatum (e-g). (a) X-ray μCT 3D images exemplifying root growth into the three key structural components considered in this study: biopores (dashed blue), macropores (> 40 μm Ø) (blue), and soil matrix (brown). Bar diagrams show relative volume fractions of these structural components under R. hirta (b) and P. virgatum growth and corresponding relative root volumes grown into them (c, f). Proportions of macropore and soil matrix components in the rhizosphere of *R. hirta* (d) and *P. virgatum* (g) are shown as a function of distance to the root surfaces, with narrow (40–150 μm Ø) and wide (> 150 μm Ø) macropores marked by orange and blue, respectively. Letters mark significant differences among the structures regarding root growth into the soil matrix and the macropores investigated by a linear mixed model. There were no significant differences in root growth into biopores.

of long-term monoculture switchgrass vegetation to increase biopore volumes (Rachman et al., 2004) was clearly pronounced, and soil from the long-term monoculture switchgrass had > 1.6 times higher biopore volumes than prairie (2.8 Vol% vs 1.7 Vol %, Fig. S3d). The differences in pores structure mainly occurred in the macropore space, while the bulk density and volumes of pores in 5–40  $\mu$ m Ø size range of the two vegetation systems were similar (Table S3).

While both plant species performed well during the 2 months of the experiment (Table S4; Fig. S1b,c), R. hirta developed significantly higher belowground biomass than P. virgatum (Table S3). Most, that is, 59–65%, of R. hirta roots grew into the soil matrix, regardless of the structure (sieved vs intact soil) or origin (switchgrass vs prairie) of the encountered soil (Fig. 2c). Only 35-45% of P. virgatum roots grew into the soil matrix when encountering the sieved soil of both origins and the intact soil of switchgrass origin (Fig. 2f). However, P. virgatum dedicated a substantially higher share of its roots (65%) to the soil matrix when growing into the intact cores of prairie origin (Fig. 2f).

Both plants markedly preferred utilising existing biopores. While biopores made up only 2-3% of the total soil volume,

18% of R. hirta roots were found in them, in switchgrass- and prairie-soils alike. P. virgatum even more distinctly preferred the biopores of its 'familiar' soil -35% of its roots grew into the biopores in the intact switchgrass-soil (Fig. 2f). Yet, a surprisingly low (only 17%) proportion of *P. virgatum* roots was found in the biopores of the intact prairie-soil.

In total, R. hirta developed >5 times greater root length density, that is, root length per volume of soil, than P. virgatum (Fig. 3a); and significantly higher total root branch density, that is, number of lateral roots per soil volume, than P. virgatum (Fig. 3b). However, when encountering the intact pore structure, both plants reacted similarly - that is, they developed significantly higher branch densities there than in the sieved soil (Fig. 3b). Further, *P. virgatum* root diameters were the smallest when growing into the intact prairie-soil, while there were no significant differences in the diameters of R. hirta roots (Fig. 3c). The mean root diameter within cores was not associated with the share of roots growing into the soil matrix (Fig. S4).

Pore connectivity appeared to play an important role in defining whether the roots grew into existing macropores and/or biopores or into the soil matrix (Fig. 3d). For both plant species and

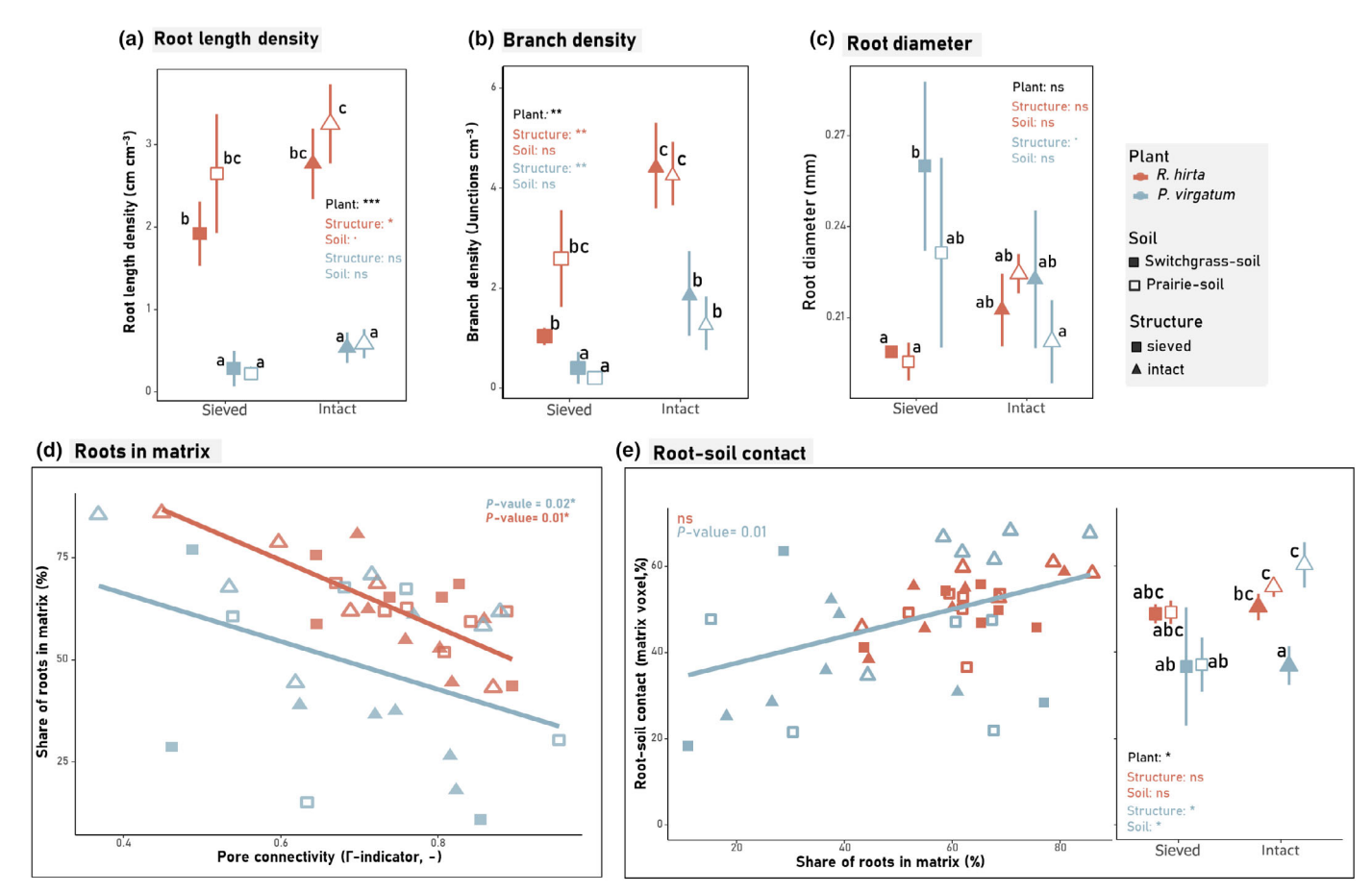


**Fig. 3** Influence of pore structure on root growth. Root length density (a), root branch density (b) and root diameter (c) of *Panicum virgatum* and *Rudbeckia hirta* when grown into sieved or intact soil of prairie or switchgrass origin. Also shown are the relationship between pore connectivity, assessed using Γ-indicator, and the share of roots growing into the soil matrix (d) and the relationship between the share of roots growing into the soil matrix and the root–soil contact (e). The mean values of root–soil contact of *P. virgatum* and *R. hirta* roots are shown when grown into sieved or intact soil of prairie or switchgrass origin (e). Note that the Γ-indicator (connection probability) is a dimensionless measure, equal to 1 for a perfectly connected pore system and 0 for a fully unconnected pore system. Root–soil contact was calculated as the percentage of matrix voxels in close proximity to the root surface (< 100 μm) and given as a mean of all roots within an ingrowth core. The solid lines represent fitted linear models. The letters indicate significant differences among the plant, structure, and soil combinations investigated by linear mixed models (*P*-value < 0.05). In addition, we report statistical significance of *F*-tests for the main effect of the plant species (*P. virgatum* vs *R. hirta*) and simple *F*-tests (aka slicing) for the effects of structure (sieved vs intact) and origin (prairie vs switchgrass-soil) within each species (shown in their respective colours) and marked by ns, \*, \*\*, and \*\*\* for *P*-values > 0.1, < 0.05, < 0.01, and < 0.001, respectively. Error bars show the SEs of the means.

in all studied pore structure systems, lower pore connectivity was associated with greater growth into the soil matrix and a subsequently increased root–soil contact (Fig. 3e). But when the roots preferentially grew into the macropores and biopores, the contact decreased. Notably, a markedly higher growth of *P. virgatum* roots into the soil matrix in the prairie-soil (Fig. 2f) corresponded to its significantly higher root–soil contact there as compared to all other soil treatments, while *R. hirta* maintained high root–soil contact throughout all pore structures (Fig. 3e).

#### Pore characteristics in root vicinity

Rhizosphere porosity was the highest in the immediate vicinity (< 100  $\mu$ m) of the roots, decreasing with the distance (Fig. 2d,g). It should be noted that narrow (40–150  $\mu$ m Ø) macropores either completely dominated the direct vicinity of the roots or constituted a substantial portion of the rhizosphere volumes there.

The plant effects on the rhizosphere porosity differed in sieved vs intact soils. In the sieved soil, the rhizosphere around  $P.\ virgatum$  roots was dominated by wide macropores (>150 µm Ø) (Fig. 2g), while narrow macropores (40–150 µm Ø) dominated the rhizosphere of  $R.\ hirta$  (Fig. 2d). In the intact soil the rhizosphere characteristics of the two plants were more similar: for both, there was a substantial presence of wide macropores in the intact switchgrass-soil and dominance of narrow macropores in the intact prairie-soil. Interestingly, only in the intact prairie-soil, where  $P.\ virgatum$  grew into the soil matrix to the same extent as  $R.\ hirta$  (Fig. 2c,f), the pore characteristics of  $P.\ virgatum$ 's rhizosphere became similar to those of  $R.\ hirta$  (Fig. 2d,g).

## Carbon translocation into the soil

Rudbeckia hirta had a higher photosynthesis rate, assimilated more <sup>14</sup>C, retained a lower proportion of assimilated <sup>14</sup>C in the shoots,

2, Dowloaded from https://nph.onlinelbrary.wiley.com/doi/10.1111/nph.19159, Wiley Online Library on [22/09/2023]. See the Terms and Conditions (https://onlinelbbrary.wiley.com/terms-and-conditions) on Wiley Online Library for rules of use; OA articles are governed by the applicable Creative Commons Licens

and transferred much more of its assimilated <sup>14</sup>C belowground than *P. virgatum* (Table S1). There was, however, a notable exception to this overall pattern: the <sup>14</sup>C allocated by *P. virgatum* into the roots and its surroundings (i.e. rhizosphere and rhizoplane) through rhizodeposition was comparable to that of *R. hirta* when *P. virgatum* grew into the intact prairie-soil (Figs 4b, S5).

It is expected that the roots actively growing at a time of a <sup>14</sup>C pulse are the ones that will be most enriched (Pausch & Kuzyakov, 2011), hence contributing the most to <sup>14</sup>C enriched rhizodeposition. However, the positive association between <sup>14</sup>C in the rhizodeposition and root–soil contact (Fig. 4a) still held even when the <sup>14</sup>C of rhizodeposits was standardised by the <sup>14</sup>C of the roots (Fig. S6). This suggests that areas of high root–soil contact were eliciting greater quantities of new C rhizodeposits from roots with a wide range of <sup>14</sup>C levels and growth stages.

The species differences in terms of the quantities of newly assimilated C transferred into the soil appeared to be driven by a greater root length density of *R. hirta* (Fig. 3a). When expressed on a per unit of root length, the newly assimilated C within the roots of the two species was similar (Fig. S7a). However, even per unit of root length, *R. hirta* translocated more of the new C into its rhizoplane than *P. virgatum* (Fig. S7b). Even though the soil origin did not influence C translocation and C soil inputs of *R. hirta*, it did matter for *P. virgatum* when grown into the prairie-soil *P. virgatum* transported in total three times more of its assimilated <sup>14</sup>C to its roots and released five times more <sup>14</sup>C in its rhizoplane than when it grew into the switchgrass-soil (Fig. S7a,b).

#### Placement and fate of photo-assimilated C in the soil

Surprisingly, despite much higher root length (Fig. 3a) and <sup>14</sup>C-activity in the roots, rhizoplane, and rhizosphere of *R. hirta* as compared to those of *P. virgatum* (Fig. 4b; Table S1), the <sup>14</sup>C activity in the grid samples of the two plants was similar (Fig. S5e). Even more surprising was that the more *P. virgatum* roots grew into the soil matrix, the lower was the <sup>14</sup>C-activity observed in the grid samples (Fig. 4g), and some of the highest grid <sup>14</sup>C corresponded to the cores where most of the *P. virgatum* roots grew into the existing biopores (Fig. 4g).

When expressed on a per unit of root length basis,  $^{14}$ C in the pore solution tended to be higher in *P. virgatum* than in *R. hirta* (Fig. S7d,e). While  $^{14}$ C-DOC from *R. hirta* was not affected by either soil structure or soil origin, we found especially high  $^{14}$ C-DOC in 2–40 µm Ø pores when *P. virgatum* grew into the intact prairie-soil, both in total and on a per unit of root length basis (Figs S5g, S7e).

Consistent with its high root biomass (Fig. 3a) and high <sup>14</sup>C rhizodepostion (Fig. 4a), *R. hirta*'s soil had significantly more <sup>14</sup>CO<sub>2</sub> emitted during the incubation than the soil of *P. virgatum* (Fig. 4d). Also, in total, more <sup>14</sup>C-SOC remained in *R. hirta*'s soil at the end of the incubation (Fig. S5d). Greater root—soil contact appeared to stimulate the processing of new C and its losses as CO<sub>2</sub>, as suggested by positive association between root—soil contact and <sup>14</sup>CO<sub>2</sub> (Fig. 4c). For both plant species roots, the higher the rhizodeposition, the more of the newly added C remained in the soil after incubation (Fig. 4e).

The degradation of roots found in the prairie-soil was roughly double that of the switchgrass-soil, equal to 67% and 34%, respectively (Fig. 5). Consistent with the positive correlations between the root–soil contact and <sup>14</sup>CO<sub>2</sub> (Fig. 4c), a positive correlation was also observed between the volumes of degraded old roots and the root–soil contact (Fig. 5a).

#### **Discussion**

Our findings suggest that for the two studied plant species, the local variations in soil pore structure influence not only the root growth patterns but also the quantities of C deposited by the roots into the soil, as well as its microbial processing. Yet, these influences depend on the root architecture of the plants. Specifically, in this study, they were negligible for the fine-root dominated *R. hirta* while major for the coarse-rooted *P. virgatum*. Greater root growth into the soil matrix enhanced root—soil contact

Root plasticity allows the plant to adapt to the changes in environmental conditions of the heterogenous soil matrix (Morris et al., 2017; Lippold et al., 2022; Glass et al., 2023). Both plants adapted their root morphology to the local structures they encountered (Fig. 3a–c). Especially *P. virgatum* created much thicker roots in the sieved cores compared to the intact structures (Fig. 3c). Roots respond to increased penetration resistance with decreasing root elongation and root thickening, which may result in a better ability to grow into denser soil matrix, while increased macroporosity was shown to have an opposite effect (Clark et al., 2003; Bengough et al., 2011; Tracy et al., 2012). However, the high water content, the bulk density of 1.34 g cm<sup>-3</sup> (Table S3) and the high macroporosity in the sieved cores make it unlikely that the roots were restricted (Jones, 1983; Valentine et al., 2012).

As expected (Stirzaker et al., 1996; Colombi et al., 2017), both plant species preferred to follow the path of least resistance and tended to choose pores with high connectivity (Fig. 3d). Lower pore connectivity stimulated root growth into the soil matrix (Fig. 3d), where greater exploration of the matrix by the roots led to stronger root-soil contact (Fig. 3e). Yet, the two species substantially differed in how they explored the soil space. Roots of R. hirta easily and readily grew into both macropores and the soil matrix, regardless of the soil structure they encountered (Fig. 2c), leading to an overall high root-soil contact. The root system of the dicot R. hirta is known for substantial quantities of lateral roots (Levang-Brilz & Biondini, 2003), a trait demonstrated when growing into the intact soil cores of this study (Fig. 3b). Laterals extending from a root located within a large pore presumably hit the surrounding soil at a nearly perpendicular angle (Jin et al., 2013) to reach water resources (Bao et al., 2014), resulting in substantial growth of R. hirta roots into the soil matrix, as observed in our study.

The pore structure encountered by the roots of *P. virgatum* had a notable influence on how it explored the soil. When *P. virgatum* encountered the pore structure created by the prairie vegetation, 65% of the small and predominately lateral roots (Fig. 3b,c) developed and grew into the soil matrix, as opposed

4698137, 2023, 2, Downloaded from https://nph.onlinelibrary.wiley.com/doi/10.1111/nph.19159, Wiley Online Library for rules of use; OA articles are governed by the applicable Cerative Commons. Licensia and Conditions (https://onlinelibrary.wiley.com/terms-and-conditions) on Wiley Online Library for rules of use; OA articles are governed by the applicable Cerative Commons. Licensia and Conditions (https://onlinelibrary.wiley.com/terms-and-conditions) on Wiley Online Library for rules of use; OA articles are governed by the applicable Cerative Commons. Licensia and Conditions (https://onlinelibrary.wiley.com/terms-and-conditions) on Wiley Online Library for rules of use; OA articles are governed by the applicable Cerative Commons. Licensia and Conditions (https://onlinelibrary.wiley.com/terms-and-conditions) on Wiley Online Library for rules of use; OA articles are governed by the applicable Cerative Commons. Licensia and Conditions (https://onlinelibrary.wiley.com/terms-and-conditions) on Wiley Online Library for rules of use; OA articles are governed by the applicable Cerative Commons. Licensia and Conditions (https://onlinelibrary.wiley.com/terms-and-conditions) on Wiley Online Library for rules of use; OA articles are governed by the applicable Cerative Commons. Licensia and Conditions (https://onlinelibrary.wiley.com/terms-and-conditions) on Wiley Online Library for rules of use; OA articles are governed by the applicable Cerative Commons. Licensia and Conditions (https://onlinelibrary.wiley.com/terms-and-conditions) on Wiley Online Library for rules of use; OA articles are governed by the applicable Cerative Commons. Licensia and Conditions (https://onlinelibrary.wiley.com/terms-and-conditions) on Wiley Online Library for rules of use; OA articles are governed by the applicable Cerative Commons. Licensia and Conditions (https://onlinelibrary.wiley.com/terms-and-conditions) on the condition of the condition

**Fig. 4** Influence of root–pore interactions on the distribution of the  $^{14}$ C label. (a) Relationships between root–soil contact and total rhizodeposition ( $^{14}$ C in the rhizosphere and rhizoplane), along with (b) corresponding mean values of the rhizodeposition in the soils of the studied structures (sieved vs intact) and origins (prairie vs switchgrass-soil). (c) Relationships between root–soil contact and the  $^{14}$ C-CO $_2$  respired during the 30-day incubation, along with (d) corresponding mean values and SEs of the  $^{14}$ C-CO $_2$  respiration. (e) Relationships between rhizodeposition and the  $^{14}$ C-SOC remaining after 30 d of incubation, along with (f) corresponding mean values and SEs of  $^{14}$ C-SOC. (g) Relationships between the share of roots growing into the soil matrix and the  $^{14}$ C in the grid samples, along with (h) corresponding mean values and SEs of grid  $^{14}$ C. The small symbols show the  $^{14}$ C activity of individual grid samples, while the large symbols represent the means for the ingrowth cores. The letters indicate significant differences among the plant, structure, and soil combinations investigated by linear mixed models (P-value < 0.05). In addition, we report statistical significance of F-tests for the main effect of the plant species (P-value < 0.05). In addition, we report statistical significance of P-tests for the main effect of the plant species (P-value < 0.05). In addition, we report statistical significance of P-tests for the main effect of the plant species (P-value < 0.05). In addition, we report statistical significance of P-tests for the main effect of the plant species (P-value < 0.05). In addition, we report statistical significance of P-tests for the main effect of the plant species (P-value < 0.05). In addition, we report statistical significance of P-tests for the main effect of the plant species (P-value < 0.05). In addition, we report statistical significance of P-tests for the main effect of the plant species (P-value < 0

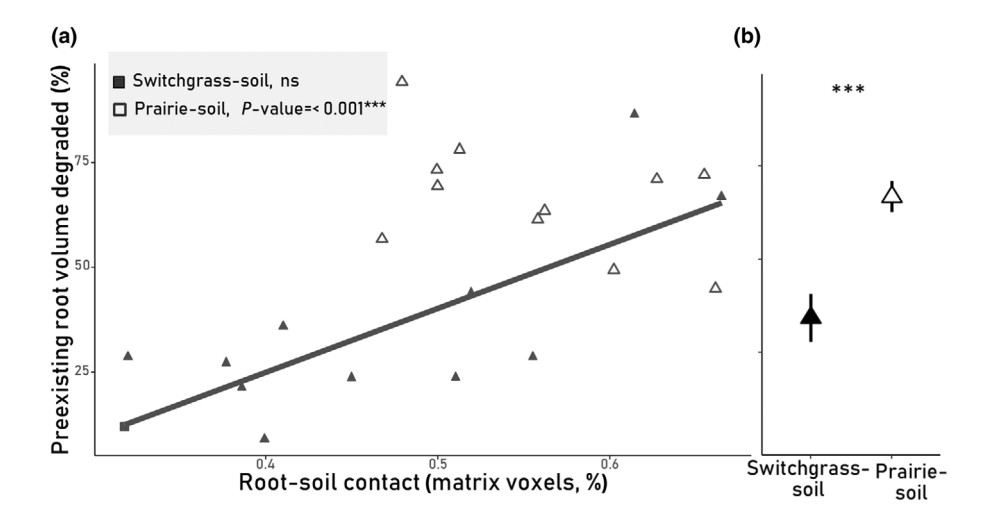


**Fig. 5** Decomposition of old root residues within the intact soil cores during the experiment. (a) Relationships between the losses in the volumes of old root residues and the root–soil contacts in the soils of switchgrass and prairie origin. The solid line represents the fitted linear model. (b) Average losses in the volumes of the old root residues in the two studied soils. Vertical lines represent SEs, and asterisk (\*\*\*) indicates the significant difference revealed by a *t*-test (*P*-value < 0.001).

to just 36–48% in all other structures (Fig. 2f) and resulting in high root–soil contact levels (Fig. 3e). On the contrary, *P. virgatum* tended to avoid the soil matrix when growing into the

other structures, that is, into sieved soils or into the intact soil of its own, that is, switchgrass origin, where it had a greater share of roots in macropores than *R. hirta* (Fig. 2c,f). Similarly,

, Downloaded from https://nph.onlinelibrary.wiley.com/doi/10.1111/nph.19159, Wiley Online Library on [22/09/2023]. See the Terms and Conditions (https://onlinelibrary.wiley.com/terms-and-conditions) on Wiley Online Library for rules of use; OA articles are governed by the applicable Creative Commons Licens

Z. maize was shown to develop a large share of lateral roots within and around loamy, dense macroaggregates, comprising only a small volume of macropores (> 40 µm), while in the otherwise sandy matrix, roots were mainly found in macropores with a low number laterals (Lippold et al., 2022). In the intact soil of the switchgrass origin, P. virgatum also had a particularly strong preference for biopores (Fig. 2f). The biopores there were most likely built by previous P. virgatum plants; thus, the newly growing roots were just following the old 'familiar' pathways (Video S1, White & Kirkegaard, 2010). Differences in root growth patterns of P. virgatum affected the pore structure of its rhizosphere (Fig. 2g). In the sieved soils of both switchgrass and prairie origin and in the intact switchgrass-soil, wide macropores prevailed in root vicinity with a concomitant significant reduction in root-soil contact (Fig. 3c).

#### Influence of roots and pores on the fate of soil C inputs

Our findings demonstrated that while soil C inputs from *R. hirta*, do not depend on the type of pore structure that is encountered by their roots (Figs 4a, S5), yet for *P. virgatum* the pore structure matters. Growth into the soil matrix and subsequently increased root—soil contact apparently influence: the amount of C released into the root's surroundings (Fig. 4a); the microbial processing of the plant-derived C (Fig. 4c); and the spatial distribution patterns of this C (Fig. 4g).

High <sup>14</sup>C-rhizodeposition of *R. hirta* coincided with a substantial portion of its extensive root system growing into the soil matrix and thus with a high root–soil contact (Fig. 4a). On the other hand, <sup>14</sup>C-rhizodeposition of *P. virgatum* was similar to that of *R. hirta* only in the intact prairie-soil, where *P. virgatum*'s roots explored the matrix as much as those of *R. hirta*. The most likely explanations of this phenomenon are: that the growth into the soil matrix requires additional mucilage production (Iijima & Kono, 1992); and that the enhanced root–soil contact increases exudation (Jones *et al.*, 2009). Our results from these two species with contrasting root systems suggest that root–soil contact might be an important driver stimulating plants to increase their C inputs (Fig. 6); however, future experimentation with a wider range of plant species will be paramount for assessing the universality of its role.

The differences in the chemical composition of the old roots of *P. virgatum* encountered in the switchgrass-soil and of the old roots of a variety of unidentified plant species in the prairie-soil were the likely important contributors to the observed difference in root decomposition of the two plants (Kim *et al.*, 2022). Yet, growth into the soil matrix and resultant greater root—soil contact also promoted microbial respiration (Fig. 4c) and root decomposition (Fig. 5). Microbial respiration depends on the spatial organisation and connectivity of pathways between decomposers and organic compounds (Nunan *et al.*, 2017; Mbé *et al.*, 2022). Root growth into the soil matrix apparently minimises distances between microbial decomposers and root-derived organic inputs, optimising the movement of labile organic compounds and enzymes (Fig. 6).

However, even when the roots grow into the soil matrix, there always remains a gap between the root and the soil surface, which can be attributed to root shrinkage (Carminati *et al.*, 2013) and to geometrical reasons, that is, the packing of round-shaped soil particles at the flat root surface (Koebernick *et al.*, 2019). Formed by narrow macropores (Fig. 2d,g), this gap can facilitate oxygen flow and greater microbial activity (van Veelen *et al.*, 2019). High abundance of narrow macropores can be particularly important for processing the newly added plant C as these pores may provide optimal micro-environmental habitats for microbial decomposers and often are characterised by greater enzyme activity and C turnover (Bouckaert *et al.*, 2013; Kravchenko *et al.*, 2019).

Spatial distribution of the plant-derived C is driven by where the plants deposit it. Thus, new C has been previously reported to be positively associated with an abundance of root-accessible macropores (Quigley *et al.*, 2018; Quigley & Kravchenko, 2022). Our results support this notion. Indeed, greater *P. virgatum* growth into the macropores corresponded to higher <sup>14</sup>C in the soil solution extracted from macropores (> 40  $\mu$ m Ø, Fig. S7d), while the highest <sup>14</sup>C in small (2–40  $\mu$ m Ø) pores was observed when *P. virgatum* grew predominately into the soil matrix (Fig. S7e).

However, surprisingly, more of *P. virgatum*'s <sup>14</sup>C was found to be ubiquitously distributed through the soil (as can be surmised from soil <sup>14</sup>C grid data) when its roots predominantly grew into the macropores (Fig. 4g). Occurrence of newly photo-assimilated C so far away from the roots could not be simply explained by diffusion away from the root-hosting macropores, as those pores were mostly air-filled during the plant growth (Schlüter et al., 2022). We propose a hypothetical explanation suggesting that the <sup>14</sup>C transport in these cases was facilitated by fungi (Fig. 6). Fungal hyphae can be important vectors of C transport into the dense soil matrix (Vidal et al., 2018; Witzgall et al., 2021). Colonisation by mycorrhiza enables a plant to gain resources from a large soil volume with relatively low C translocation into the soil (Veresoglou et al., 2012). Fungi grow preferentially into larger (> 100 μm), air-filled pores (Otten et al., 2001; Soufan et al., 2018), and their growth is stimulated by greater pore volume and connectivity (Erktan et al., 2020). Preferential root growth into such well-connected macropores (Fig. 3c) presumably provided ideal conditions for fungal hyphae colonisation and respective food chain for the distribution of C products throughout the soil. Mycorrhiza fungi can have a large positive effect on P. virgatum growth (Hestrin et al., 2021), and their presence in the biopores of the switchgrass-soil might compensate for decreased root growth and low root-soil contact and facilitate aboveground plant growth (Schroeder-Moreno et al., 2012). Interestingly, P. virgatum seemed not only to modify its C inputs into the rhizoplane depending on the encountered pore structure but also apparently changed the relationships with the microbial community of the surrounding soil - possibly, relying more on the bacterial activity in its immediate rhizosphere when the rootsoil contact was good while utilising the extended fungal network when the root-soil contact was poor. Future experimental work will be needed to test this hypothesis.

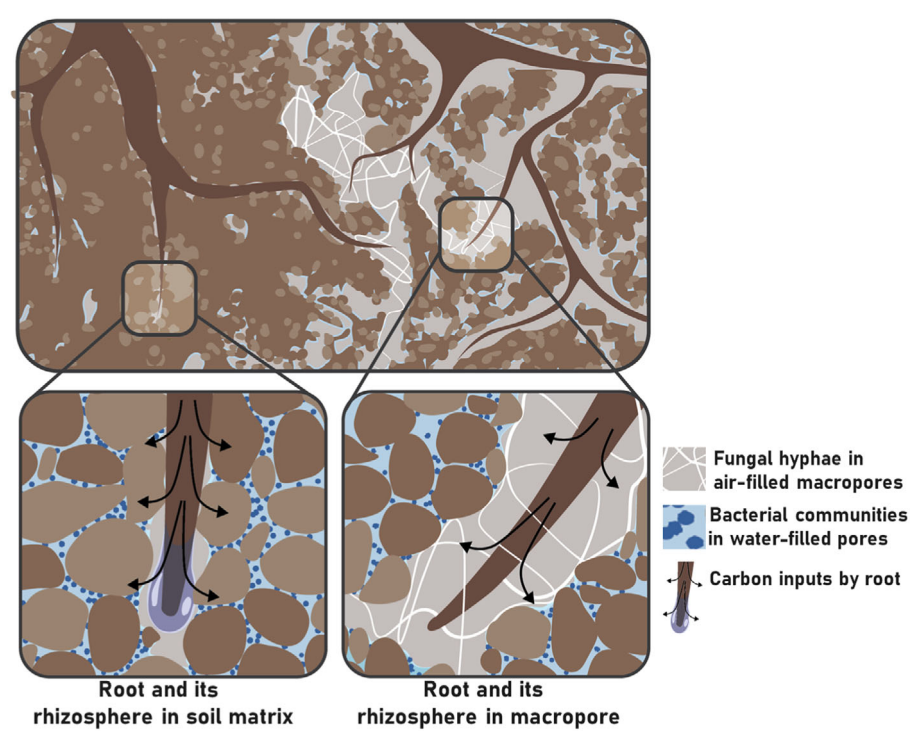


**Fig. 6** Conceptual model relating root growth patterns with pore characteristics and the fate of C, developed based on the observations from the two studied plant species. As roots grow, they produce exudates to facilitate the procurement of nutrients, build beneficial microbial communities, and optimise water supply (Hinsinger *et al.*, 2009; Nguyen, 2009). The roots also produce mucilage, rich in a variety of organic compounds and released, along with exudates, by the growing root into its surroundings (Hinsinger *et al.*, 2009; Jones *et al.*, 2009; Young & Bengough, 2018). Roots growing into the soil matrix generate greater C inputs compared to the roots growing into macro- and biopores. The reasons for this are the need for mucilage to enable the root to move through dense soil material (lijima & Kono, 1992; Young, 1998) and an increased exudation due to the enhanced root–soil contact (Jones *et al.*, 2009). The roots also modify their interactions with soil microorganisms depending on the pore structure they must navigate through (Young & Bengough, 2018). When growing into the soil matrix, roots increase exudation to attract microorganisms in their immediate vicinity and enable direct nutrient uptake. When growing into wide macro- and biopores they may rely more on symbiotic fungal networks to explore the surrounding soil. In the case of roots growing through the soil matrix, greater plant-derived C inputs, when the root is alive, and greater decomposition upon root's death create a zone of high microbial activity. Moreover, the root growing through the soil matrix also creates an optimal pore structure for long-term C storage in its rhizosphere, which facilitates greater diffusion of decomposition products into the small pores of the nearby surroundings. In the case of roots growing into macro- and biopores, only relatively small quantities of C are passed directly from the roots into fungal hyphae and further into the surrounding soil, yet without enriching the immediate rhizosphere.

Although root growth into the soil matrix and the subsequently increased root—soil contact (Fig. 3d) apparently benefited plant residue decomposition (Fig. 5) and C losses (Fig. 4c), the good root—soil contact was still advantageous for photo-assimilated C to remain protected in the soil, as attested by our 30-d incubation results (Fig. 4e). Processing of the new C inputs by microorganisms and subsequent conversion of the decomposition products into mineral-associated organic C is one important pathway of soil C gains (Cotrufo *et al.*, 2015), while direct stabilisation of plant inputs or microbial extracellular products and necromass is the other major route (Craig *et al.*, 2022).

However, regardless of the stabilisation pathway, the long-term storage potential of the newly added C depends on protection from further decomposition (Schmidt *et al.*, 2011; Dungait *et al.*, 2012). Enhanced root—soil contact increases microbial respiration (Fig. 4c), but it also enables larger quantities of root-derived C products to diffuse into the dense soil matrix surrounding the plant roots (Fig. 2d,g, also demonstrated in Schlüter *et al.*, 2022). Much longer incubation times than the typical 30-d employed by our study would be needed to quantify the long-term C storage. Yet,

the rhizosphere is known to densify upon subsequent root growth, with its porosity and permeability being reduced, while binding opportunities for C compounds increase (van Veelen *et al.*, 2019), therefore providing optimal settings for creating mineral-associated organic matter for long-term storage (Fig. 6).

## Concluding remarks and general implications

Comparisons between sieved switchgrass and prairie-soils enabled us to assess the role of non-structural effects, that is, the inherent differences in chemical and microbial properties. In the studied soil (silt-loam Alfisol), the non-structural effects were of no consequence for *R. hirta*'s root growth and inputs and played only a minor role for *P.virgatum* (Figs 3, 4, S5).

Comparisons between sieved and intact soils enabled us to assess the role of the structural effects. The strength of the structural effect depended on the plant species and on the soil's origin/vegetation history (Figs 4, S5): it was negligible for *R.hirta* in both soils, and it also was unsubstantial in the switchgrass-soil for both plants. Yet, in the prairie-soil the structural effect played a

2, Downloaded from https://hph.onlinelibrary.wiley.com/doi/10.1111/nph.19159, Wiley Online Library on [22/09/2023]. See the Terms and Conditions (https://onlinelibrary.wiley.com/terms-and-conditions) on Wiley Online Library for rules of use; OA articles are governed by the applicable Cerative Commons. License and Conditions (https://onlinelibrary.wiley.com/terms-and-conditions) on Wiley Online Library for rules of use; OA articles are governed by the applicable Cerative Commons. License and Conditions (https://onlinelibrary.wiley.com/terms-and-conditions) on Wiley Online Library for rules of use; OA articles are governed by the applicable Cerative Commons. License and Conditions (https://onlinelibrary.wiley.com/terms-and-conditions) on Wiley Online Library for rules of use; OA articles are governed by the applicable Cerative Commons. License and Conditions (https://onlinelibrary.wiley.com/terms-and-conditions) on Wiley Online Library for rules of use; OA articles are governed by the applicable Cerative Commons. License and Conditions (https://onlinelibrary.wiley.com/terms-and-conditions) on Wiley Online Library for rules of use; OA articles are governed by the applicable Cerative Commons. License and Conditions (https://onlinelibrary.wiley.com/terms-and-conditions) on Wiley Online Library for rules of use; OA articles are governed by the applicable Cerative Commons. License and Conditions (https://onlinelibrary.wiley.com/terms-and-conditions) on Wiley Online Library for rules of use; OA articles are governed by the applicable Cerative Commons. License are governed by the applicable Cerative Commons are governed by the applicable Cerative Commons. License are governed by the applicable Cerative Commons are governed by the applica

major role for *P. virgatum* in terms of its influence on where the roots grew and how much C they placed into the soil. When the pore structure of the intact prairie-soil was destroyed by sieving, P. virgatum's growth patterns, root-derived C inputs, and their processing changed dramatically. Our findings contribute to the explanation of an apparent paradox of P. virgatum being a positive influence on C gains in polyculture systems (Yang et al., 2019), while demonstrating a very slow, at best, C accrual as a monoculture (Kantola et al., 2017; Chatterjee et al., 2018), despite its extensive root system (McLaughlin & Adams Kszos, 2005; Chimento et al., 2016). Plant community of restored prairie with its diverse root systems establish a broad PSD with fewer large biopores (Fig. S1c,d, Bodner et al., 2014), arguably an ideal pore structure for C sequestration. When encountering that structure, the roots of P. virgatum were not trapped within wide macropores (as was the case when they grew into the switchgrass-soil), but explored the soil matrix, maintained good root-soil contact, with subsequent soil C input and protection benefits (Figs 3, 4).

The use of the ingrowth cores within large pots enabled us to follow the root growth of a single plant into different structures with high resolution and to capture a large part of the total root system. While this work should be followed by further experiments with a wide range of plant species and soils, consistently high inputs of root-derived C from *R. hirta* across all studied soil structures indicate the possibility of stimulating soil C gains by cultivating plants with certain root characteristics. Root systems that maintain high root–soil contact can potentially improve C accumulation across a wide range of soil pore structures.

## **Acknowledgements**

This research was funded in part by the Great Lakes Bioenergy Research Center, US Department of Energy, Office of Science, Office of Biological and Environmental Research under award no. DE-SC0018409, by the NSF DEB Program (award no. 1904267), by the NSF LTER Program (DEB 1027253) at the Kellogg Biological Station, and by Michigan State University AgBioResearch.

We thank Maxwell Oerther for his great support during the whole experiment, Jinho Lee for his help on the field site and soil chemical analysis and Michelle Quigley for her support during the X-ray CT scans. We are indebted to Chelsea Mamott of the GLBRC communication team for the artwork. We highly appreciate the help from the laboratories of Eric Patterson and Thomas Sharkey during the <sup>14</sup>C analysis and <sup>14</sup>C labelling, respectively.

We thank GeoSoilEnviroCARS (The University of Chicago, Sector 13), Advanced Photon Source (APS), Argonne National Laboratory, and most notably, M. L. Rivers for the possibility and assistance with synchrotron CT measurements. We thank the anonoymous reviewers for their suggestions, which greatly improved the manuscript.

## **Competing interests**

None declared.

#### **Author contributions**

ML and JPS labelled the plants. JC and ML analysed the <sup>14</sup>C labelled plant and soil samples. AG and ML constructed and built the plant pots, ingrowth cores and cores for collecting soil water. ML, AK and AG designed the experimental setup. All authors discussed the results and finalised the paper. AK and ML analysed the structure and wrote the paper.

#### **ORCID**

Jinyi Chen https://orcid.org/0000-0002-4594-254X
Andrey Guber https://orcid.org/0000-0002-0277-5227
Alexandra Kravchenko https://orcid.org/0000-0001-5920-927X

Maik Lucas https://orcid.org/0000-0002-4287-7666 James P. Santiago https://orcid.org/0000-0002-4186-8303

## Data availability

All raw data that support this study are available under doi: 10. 48758/ufz.13657.

#### References

Bao Y, Aggarwal P, Robbins NE, Sturrock CJ, Thompson MC, Tan HQ, Tham C, Duan L, Rodriguez PL, Vernoux T et al. 2014. Plant roots use a patterning mechanism to position lateral root branches toward available water. Proceedings of the National Academy of Sciences, USA 111: 9319–9324.

Bates D, Mächler M, Bolker B, Walker S. 2015. Fitting linear mixed-effects models using LME4. *Journal of Statistical Software* 67: 1–48.

Bengough AG, McKenzie BM, Hallett PD, Valentine TA. 2011. Root elongation, water stress, and mechanical impedance: a review of limiting stresses and beneficial root tip traits. *Journal of Experimental Botany* 62: 59–68

Bodner G, Leitner D, Kaul H-P. 2014. Coarse and fine root plants affect pore size distributions differently. *Plant and Soil* 380: 133–151.

Bouckaert L, Sleutel S, van Loo D, Brabant L, Cnudde V, van Hoorebeke L, de Neve S, 2013. Carbon mineralisation and pore size classes in undisturbed soil cores. Soil Research 51: 14.

Bruand A, Cousin I, Niccoullaud B, Duval O, Begon JC. 1996. Backscattered electron scanning images of soil porosity for analyzing soil compaction around roots. Soil Science Society of America Journal 60: 895–901.

Buades A, Coll B, Morel J-M. 2011. Non-local means denoising. *Image Processing on Line* 1: 208–212.

Carminati A, Vetterlein D, Koebernick N, Blaser S, Weller U, Vogel H-J. 2013. Do roots mind the gap? *Plant and Soil* 367: 651–661.

Chatterjee A, Long DS, Pierce FJ. 2018. Change in soil organic carbon after five years of continuous winter wheat or switchgrass. Soil Science Society of America Journal 82: 332–342.

Chimento C, Almagro M, Amaducci S. 2016. Carbon sequestration potential in perennial bioenergy crops: the importance of organic matter inputs and its physical protection. *GCB Bioenergy* 8: 111–121.

Clark LJ, Whalley WR, Barraclough PB. 2003. How do roots penetrate strong soil? *Plant and Soil* 255: 93–104.

Colombi T, Braun S, Keller T, Walter A. 2017. Artificial macropores attract crop roots and enhance plant productivity on compacted soils. Science of the Total Environment 574: 1283–1293.

Colombi T, Torres LC, Walter A, Keller T. 2018. Feedbacks between soil penetration resistance, root architecture and water uptake limit water accessibility and crop growth – a vicious circle. *Science of the Total Environment* 626: 1026–1035.

- Colombi T, Walder F, Büchi L, Sommer M, Liu K, Six J, van der Heijden MGA, Charles R, Keller T. 2019. On-farm study reveals positive relationship between gas transport capacity and organic carbon content in arable soil. *The Soil* 5: 91–105.
- Cotrufo MF, Soong JL, Horton AJ, Campbell EE, Haddix ML, Wall DH, Parton WJ. 2015. Formation of soil organic matter via biochemical and physical pathways of litter mass loss. *Nature Geoscience* 8: 776–779.
- Craig ME, Geyer KM, Beidler KV, Brzostek ER, Frey SD, Stuart Grandy A, Liang C, Phillips RP. 2022. Fast-decaying plant litter enhances soil carbon in temperate forests but not through microbial physiological traits. *Nature Communications* 13: 1229.
- Darbon J, Cunha A, Chan TF, Osher S, Jensen GJ. 2008. Fast nonlocal filtering applied to electron cryomicroscopy. In: 2008 5<sup>th</sup> IEEE international symposium on biomedical imaging: from nano to macro. Paris, France: IEEE, 1331–1334.
- Dexter AR. 1991. Amelioration of soil by natural processes. *Soil and Tillage Research* 20: 87–100.
- **Domander R, Felder AA, Doube M. 2021.** BONE J2 refactoring established research software. *Wellcome Open Research* **6**: 37.
- Dungait JAJ, Hopkins DW, Gregory AS, Whitmore AP. 2012. Soil organic matter turnover is governed by accessibility not recalcitrance. Global Change Biology 18: 1781–1796.
- Erktan A, Or D, Scheu S. 2020. The physical structure of soil: determinant and consequence of trophic interactions. *Soil Biology and Biochemistry* 148: 107876.
- Friedlingstein P, O'Sullivan M, Jones MW, Andrew RM, Gregor L, Hauck J, Le Quéré C, Luijkx IT, Olsen A, Peters GP et al. 2022. Global carbon budget 2022. Earth System Science Data 14: 4811–4900.
- Gao W, Hodgkinson L, Jin K, Watts CW, Ashton RW, Shen J, Ren T, Dodd IC, Binley A, Phillips AL et al. 2016. Deep roots and soil structure. Plant, Cell & Environment 39: 1662–1668.
- Gherardi LA, Sala OE. 2020. Global patterns and climatic controls of belowground net carbon fixation. *Proceedings of the National Academy of Sciences, USA* 117: 20038–20043.
- Glass NT, Yun K, Dias de Oliveira EA, Zare A, Matamala R, Kim S-H, Gonzalez-Meler M. 2023. Perennial grass root system specializes for multiple resource acquisitions with differential elongation and branching patterns. Frontiers in Plant Science 14: 1146681.
- Gregory PJ. 2022. Russell review: are plant roots only "in" soil or are they "of" it? Roots, soil formation and function. *European Journal of Soil Science* 73: e13219.
- Hestrin R, Lee MR, Whitaker BK, Pett-Ridge J. 2021. The switchgrass microbiome: a review of structure, function, and taxonomic distribution. *Phytobiomes Journal* 5: 14–28.
- Hildebrand T, Rüegsegger P. 1997. A new method for the model-independent assessment of thickness in three-dimensional images. *Journal of Microscopy* 185: 67–75.
- Hinsinger P, Bengough AG, Vetterlein D, Young IM. 2009. Rhizosphere: biophysics, biogeochemistry and ecological relevance. *Plant and Soil* 321: 117–152.
- Iijima M, Kono Y. 1992. Development of golgi apparatus in the root cap cells of maize (*Zea mays* L.) as affected by compacted soil. *Annals of Botany* 70: 207– 212.
- Jin K, Shen J, Ashton RW, Dodd IC, Parry MAJ, Whalley WR. 2013. How do roots elongate in a structured soil? *Journal of Experimental Botany* 64: 4761– 4777.
- Jones CA. 1983. Effect of soil texture on critical bulk densities for root growth. Soil Science Society of America Journal 47: 1208.
- Jones DL, Nguyen C, Finlay RD. 2009. Carbon flow in the rhizosphere: carbon trading at the soil–root interface. *Plant and Soil* 321: 5–33.
- Judd LA, Jackson BE, Fonteno WC. 2015. Rhizometer: an apparatus to observe and measure root growth and its effect on container substrate physical properties over time. *HortScience* 50: 288–294.
- Juyal A, Guber A, Oerther M, Quigley M, Kravchenko A. 2021. Pore architecture and particulate organic matter in soils under monoculture switchgrass and restored prairie in contrasting topography. *Scientific Reports* 11: 21998.

- Kantola IB, Masters MD, DeLucia EH. 2017. Soil particulate organic matter increases under perennial bioenergy crop agriculture. Soil Biology and Biochemistry 113: 184–191.
- Kim K, Gil J, Ostrom NE, Gandhi H, Oerther MS, Kuzyakov Y, Guber AK, Kravchenko AN. 2022. Soil pore architecture and rhizosphere legacy define N<sub>2</sub>O production in root detritusphere. Soil Biology and Biochemistry 166: 108565
- Klein S, Staring M, Murphy K, Viergever MA, Pluim J. 2010. ELASTIX: a toolbox for intensity-based medical image registration. *IEEE Transactions on Medical Imaging* 29: 196–205.
- Koebernick N, Daly KR, Keyes SD, Bengough AG, Brown LK, Cooper LJ, George TS, Hallett PD, Naveed M, Raffan A et al. 2019. Imaging microstructure of the barley rhizosphere: particle packing and root hair influences. New Phytologist 221: 1878–1889.
- Koebernick N, Schlüter S, Blaser SRGA, Vetterlein D. 2018. Root-soil contact dynamics of Vicia faba in sand. Plant and Soil 431: 417–431.
- Kravchenko AN, Guber AK. 2017. Soil pores and their contributions to soil carbon processes. *Geoderma* 287: 31–39.
- Kravchenko AN, Guber AK, Razavi BS, Koestel J, Quigley MY, Robertson GP, Kuzyakov Y. 2019. Microbial spatial footprint as a driver of soil carbon stabilization. *Nature Communications* 10: 3121.
- Levang-Brilz N, Biondini ME. 2003. Growth rate, root development and nutrient uptake of 55 plant species from the Great Plains Grasslands, USA. *Plant Ecology* 165: 117–144.
- Lippold E, Lucas M, Fahrenkampf T, Schlüter S, Vetterlein D. 2022.

  Macroaggregates of loam in sandy soil show little influence on maize growth, due to local adaptations of root architecture to soil heterogeneity. *Plant and Soil* 478: 163–175.
- Lucas M. 2022. Perspectives from the Fritz–Scheffer Awardee 2020 the mutual interactions between roots and soil structure and how these affect rhizosphere processes. *Journal of Plant Nutrition and Soil Science* 185: 8–18.
- Lucas M, Balbín-Suárez A, Smalla K, Vetterlein D. 2018. Root growth, function and rhizosphere microbiome analyses show local rather than systemic effects in apple plant response to replant disease soil. *PLoS ONE* 13: e0204922.
- Lucas M, Nguyen LTT, Guber A, Kravchenko AN. 2022. Cover crop influence on pore size distribution and biopore dynamics: enumerating root and soil faunal effects. Frontiers in Plant Science 13: 928569.
- Lucas M, Pihlap E, Steffens M, Vetterlein D, Kögel-Knabner I. 2020a.

  Combination of imaging infrared spectroscopy and X-ray computed microtomography for the investigation of bio- and physicochemical processes in structured soils. Frontiers in Environmental Science 8: 42.
- Lucas M, Schlüter S, Vogel H-J, Vetterlein D. 2019a. Roots compact the surrounding soil depending on the structures they encounter. *Scientific Reports* 9: 16236.
- Lucas M, Schlüter S, Vogel H-J, Vetterlein D. 2019b. Soil structure formation along an agricultural chronosequence. *Geoderma* 350: 61–72.
- Lucas M, Vetterlein D, Vogel H-J, Schlüter S. 2020b. Revealing pore connectivity across scales and resolutions with X-ray CT. European Journal of Soil Science 72: 546–560.
- Mbé B, Monga O, Pot V, Otten W, Hecht F, Raynaud X, Nunan N, Chenu C, Baveye PC, Garnier P. 2022. Scenario modelling of carbon mineralization in 3D soil architecture at the microscale: toward an accessibility coefficient of organic matter for bacteria. European Journal of Soil Science 73: e13144.
- McLaughlin SB, Adams Kszos L. 2005. Development of switchgrass (*Panicum virgatum*) as a bioenergy feedstock in the United States. *Biomass and Bioenergy* 28: 515–535.
- Morris EC, Griffiths M, Golebiowska A, Mairhofer S, Burr-Hersey J, Goh T, Von Wangenheim D, Atkinson B, Sturrock CJ, Lynch JP *et al.* 2017. Shaping 3D root system architecture. *Current Biology* 27: R919–R930.
- Nguyen C. 2009. Rhizodeposition of organic C by plant: mechanisms and controls. In: Lichtfouse E, Navarrete M, Debaeke P, Véronique S, Alberola C, eds. Sustainable agriculture. Dordrecht, the Netherlands: Springer Netherlands, 97–123.
- Nunan N, Leloup J, Ruamps LS, Pouteau V, Chenu C. 2017. Effects of habitat constraints on soil microbial community function. Scientific Reports 7: 4280.

2, Downloaded from https://hph.onlinelibrary.wiley.com/doi/10.1111/nph.19159, Wiley Online Library on [22/09/2023]. See the Terms and Conditions (https://onlinelibrary.wiley.com/terms-and-conditions) on Wiley Online Library for rules of use; OA articles are governed by the applicable Cerative Commons. License and Conditions (https://onlinelibrary.wiley.com/terms-and-conditions) on Wiley Online Library for rules of use; OA articles are governed by the applicable Cerative Commons. License and Conditions (https://onlinelibrary.wiley.com/terms-and-conditions) on Wiley Online Library for rules of use; OA articles are governed by the applicable Cerative Commons. License and Conditions (https://onlinelibrary.wiley.com/terms-and-conditions) on Wiley Online Library for rules of use; OA articles are governed by the applicable Cerative Commons. License and Conditions (https://onlinelibrary.wiley.com/terms-and-conditions) on Wiley Online Library for rules of use; OA articles are governed by the applicable Cerative Commons. License and Conditions (https://onlinelibrary.wiley.com/terms-and-conditions) on Wiley Online Library for rules of use; OA articles are governed by the applicable Cerative Commons. License and Conditions (https://onlinelibrary.wiley.com/terms-and-conditions) on Wiley Online Library for rules of use; OA articles are governed by the applicable Cerative Commons. License and Conditions (https://onlinelibrary.wiley.com/terms-and-conditions) on Wiley Online Library for rules of use; OA articles are governed by the applicable Cerative Commons. License are governed by the applicable Cerative Commons are governed by the applicable Cerative Commons. License are governed by the applicable Cerative Commons are governed by the applica

- Otsu N. 1979. A threshold selection method from gray-level histograms. *IEEE Transactions on Systems, Man and Cybernetics* 9: 62–66.
- Otten W, Hall D, Harris K, Ritz K, Young IM, Gilligan CA. 2001. Soil physics, fungal epidemiology and the spread of *Rhizoctonia solani*. New Phytologist 151: 459–468
- Pausch J, Kuzyakov Y. 2011. Photoassimilate allocation and dynamics of hotspots in roots visualized by <sup>14</sup>C phosphor imaging. *Journal of Plant Nutrition and Soil Science* 174: 12–19.
- Pausch J, Kuzyakov Y. 2018. Carbon input by roots into the soil: quantification of rhizodeposition from root to ecosystem scale. Global Change Biology 24: 1– 12.
- Poeplau C, Don A, Schneider F. 2021. Roots are key to increasing the mean residence time of organic carbon entering temperate agricultural soils. *Global Change Biology* 27: 4921–4934.
- Poirier V, Roumet C, Munson AD. 2018. The root of the matter: linking root traits and soil organic matter stabilization processes. Soil Biology and Biochemistry 120: 246–259.
- Quigley MY, Kravchenko AN. 2022. Inputs of root-derived carbon into soil and its losses are associated with pore-size distributions. *Geoderma* 410: 115667.
- Quigley MY, Negassa WC, Guber AK, Rivers ML, Kravchenko AN. 2018. Influence of pore characteristics on the fate and distribution of newly added carbon. Frontiers in Environmental Science 6: 868.
- Rabot E, Wiesmeier M, Schlüter S, Vogel H-J. 2018. Soil structure as an indicator of soil functions: a review. *Geoderma* 314: 122–137.
- Rachman A, Anderson SH, Gantzer CJ, Alberts EE. 2004. Soil hydraulic properties influenced by stiff-stemmed grass hedge systems. Soil Science Society of America Journal 68: 1386–1393.
- Rasse DP, Rumpel C, Dignac M-F. 2005. Is soil carbon mostly root carbon? Mechanisms for a specific stabilisation. *Plant and Soil* 269: 341–356.
- van Rossum G, Drake FL. 2009. *PYTHON 3 reference manual*. Scotts Valley, CA, USA: CreateSpace.
- Russell MB, Richards LA. 1939. The determination of soil moisture energy relations by centrifugation. Soil Science Society of America Journal 3: 65–69.
- Santiago JP, Soltani A, Bresson MM, Preiser AL, Lowry DB, Sharkey TD. 2021. Contrasting anther glucose-6-phosphate dehydrogenase activities between two bean varieties suggest an important role in reproductive heat tolerance. *Plant, Cell & Environment* 44: 2185–2199.
- Schlüter S, Leuther F, Albrecht L, Hoeschen C, Kilian R, Surey R, Mikutta R, Kaiser K, Mueller CW, Vogel H-J. 2022. Microscale carbon distribution around pores and particulate organic matter varies with soil moisture regime. Nature Communications 13: 2098.
- Schmidt MWI, Torn MS, Abiven S, Dittmar T, Guggenberger G, Janssens IA,
   Kleber M, Kögel-Knabner I, Lehmann J, Manning DAC et al. 2011.
   Persistence of soil organic matter as an ecosystem property. Nature 478: 49–56.
- Schroeder-Moreno MS, Greaver TL, Wang S, Hu S, Rufty TW. 2012. Mycorrhizal-mediated nitrogen acquisition in switchgrass under elevated temperatures and N enrichment. *GCB Bioenergy* 4: 266–276.
- Shamonin D. 2013. Fast parallel image registration on CPU and GPU for diagnostic classification of Alzheimer's disease. Frontiers in Neuroinformatics 7: 50.
- Sokol NW, Kuebbing SE, Karlsen-Ayala E, Bradford MA. 2019. Evidence for the primacy of living root inputs, not root or shoot litter, in forming soil organic carbon. *New Phytologist* 221: 233–246.
- Soufan R, Delaunay Y, Gonod LV, Shor LM, Garnier P, Otten W, Baveye PC. 2018. Pore-scale monitoring of the effect of microarchitecture on fungal growth in a two-dimensional soil-like micromodel. Frontiers in Environmental Science 6: 68.
- Stirzaker RJ, Passioura JB, Wilms Y. 1996. Soil structure and plant growth: Impact of bulk density and biopores. *Plant and Soil* 185: 151–162.
- Tracy SR, Black CR, Roberts JA, Sturrock C, Mairhofer S, Craigon J, Mooney SJ. 2012. Quantifying the impact of soil compaction on root system architecture in tomato (*Solanum lycopersicum*) by X-ray micro-computed tomography. *Annals of Botany* 110: 511–519.

- Valentine TA, Hallett PD, Binnie K, Young MW, Squire GR, Hawes C, Bengough AG. 2012. Soil strength and macropore volume limit root elongation rates in many UK agricultural soils. *Annals of Botany* 110: 259–270.
- van Veelen A, Koebernick N, Scotson CS, McKay-Fletcher D, Huthwelker T, Borca CN, Mosselmans JFW, Roose T. 2019. Root-induced soil deformation influences Fe, S and P: rhizosphere chemistry investigated using synchrotron XRF and XANES. *New Phytologist* 225: 1476–1490.
- Veresoglou SD, Menexes G, Rillig MC. 2012. Do arbuscular mycorrhizal fungi affect the allometric partition of host plant biomass to shoots and roots? A meta-analysis of studies from 1990 to 2010. *Mycorrhiza* 22: 227–235.
- Vetterlein D, Carminati A, Kögel-Knabner I, Bienert GP, Smalla K, Oburger E, Schnepf A, Banitz T, Tarkka MT, Schlüter S. 2020. Rhizosphere spatiotemporal organization a key to rhizosphere functions. *Frontiers in Agronomy* 2: 8.
- Vidal A, Hirte J, Bender SF, Mayer J, Gattinger A, Höschen C, Schädler S, Iqbal TM, Mueller CW. 2018. Linking 3D soil structure and plant-microbesoil carbon transfer in the rhizosphere. *Frontiers in Environmental Science* 6: 9.
- van der Walt S, Schönberger JL, Nunez-Iglesias J, Boulogne F, Warner JD, Yager N, Gouillart E, Yu T. 2014. SCIKIT-IMAGE: image processing in PYTHON. Perr J 2: e453
- Weaver JE. 1968. Prairie plants and their environment. *Papers of John E. Weaver* (1884–1956). 8.
- White RG, Kirkegaard JA. 2010. The distribution and abundance of wheat roots in a dense, structured subsoil implications for water uptake. *Plant, Cell & Environment* 33: 133–148.
- Witzgall K, Vidal A, Schubert DI, Höschen C, Schweizer SA, Buegger F, Pouteau V, Chenu C, Mueller CW. 2021. Particulate organic matter as a functional soil component for persistent soil organic carbon. *Nature Communications* 12: 4115.
- Yang Y, Tilman D, Furey G, Lehman C. 2019. Soil carbon sequestration accelerated by restoration of grassland biodiversity. *Nature Communications* 10: 718
- Young IM. 1998. Biophysical interactions at the root–soil interface: a review. *The Journal of Agricultural Science* 130: 1–7.
- Young IM, Bengough AG. 2018. The search for the meaning of life in soil: an opinion. *European Journal of Soil Science* 69: 31–38.

# **Supporting Information**

Additional Supporting Information may be found online in the Supporting Information section at the end of the article.

- **Fig. S1** Photographs taken during the plant growth and after plant harvest.
- **Fig. S2** Relationship of root length densities estimated with X-ray  $\mu$ CT and disturbed.
- **Fig. S3** Pore characteristics of the cores with intact or sieved soils of switchgrass or prairie origin before plant growth.
- **Fig. S4** Pore characteristics of the cores with intact or sieved soils of switchgrass or prairie origin before plant growth.
- **Fig. S5** Distribution of <sup>14</sup>C in intact and sieved cores of the switchgrass and prairie origin subjected to *Panicum virgatum* and *Rudbeckia hirta* growth.
- **Fig. S6** Relationship between root–soil contact and the ratio of <sup>14</sup>C in rhizodeposition and <sup>14</sup>C in roots.

**Fig. S7** Distribution of <sup>14</sup>C between the different compartments expressed on per unit of root length.

Methods S1 MLE Site and soil handling.

Methods S2 Plant growing conditions.

Methods S3 Radioactivity evaluation.

**Methods S4** Validating root segmentation by destructive sampling.

Methods S5 Analyse of subsamples at Argonne national lab for pores  $\! \leq \! 40 \; \mu m.$ 

**Table S1** <sup>14</sup>C Labelling of the plants and translocation of the <sup>14</sup>C label into shoots, roots, rhizoplane, and rhizosphere of *Rudbeckia hirta* and *Panicum virgatum*.

**Table S2** Selected chemical properties of the soils under monoculture switchgrass and restored prairie vegetation systems.

**Table S3** Selected physical properties of the soils under monoculture switchgrass and restored prairie vegetation systems.

**Table S4** Root and shoot weights for the two investigated plant species and corresponding root: shoot ratios.

**Video S1** Visualisation of root growth through different soil components.

Please note: Wiley is not responsible for the content or functionality of any Supporting Information supplied by the authors. Any queries (other than missing material) should be directed to the *New Phytologist* Central Office.